

Preparation and dielectric properties of copper phthalocyanine/graphene oxide nanohybrids via in situ polymerization

Zicheng Wang¹ · Renbo Wei¹ · Xiaobo Liu¹

Received: 18 November 2015 / Accepted: 25 January 2016 / Published online: 3 February 2016
© Springer Science+Business Media New York 2016

Abstract A novel copper phthalocyanine-grafted graphene oxide (CuPc-g-GO) nanohybrid was prepared via in situ polymerization. Isophorone diisocyanate (IPDI) and 3-aminophenoxypthalonitrile were employed to functionalize GO with phthalonitrile moieties (GO-IPDI-CN), which was subsequently polymerized with 1,3,5-tri-(3,4-dicyanophenoxy) benzene and CuCl, forming the copper phthalocyanine between the sheets of GO. The CuPc-g-GO and the intermediates were characterized by FTIR, TGA, DSC, XPS, SEM, UV-Vis, XRD, and AFM. The results suggested that CuPc was successfully grafted on the surface of GO, and the GO was completely exfoliated after the grafting of the CuPc. And the formation of the nanohybrids effectively enhanced the dielectric constant of CuPc, which was as high as 9.04 at 100 Hz, with an increment of 116 %, when the mass fraction of GO-IPDI-CN was 10 wt%.

Introduction

Graphene oxide (GO), two-dimensional sheet of covalently bonded carbon atoms, contains versatile oxygen functional groups (hydroxyl, epoxide, and carbonyl groups) on the basal planes and edges [1]. The presence of oxygen functional groups endows GO with strong polarity, which not only effectively improves the interfacial interaction between GO and polymer matrixes, but also significantly enhances the compatibility of GO in the polymer matrixes. Meanwhile, those oxygen functional groups on the GO surface provide abundant reaction sites for further chemical functionalization [1]. Hence, GO exhibits great potential for improving the properties of polymer through covalent grafting [2–6] or physical blending/absorption [7–9] due to its extremely high aspect ratio, unique graphitized planar structure, and low manufacturing costs.

Copper phthalocyanine (CuPc) and/or phthalocyanine derivatives have attracted considerable interest owing to their unique structural characteristics, synthetic method, and large number of functional end-groups (–CN) [10–12]. In addition to the obvious attractiveness of the studies for basic science, CuPc and its derivatives have many potential applications including serving as the building block for the fabrication of solar cell, fuel cells, optical-limiting materials, gas sensors, and field-effect transistors [13–16]. Among these applications, the dielectric property is one of the most important parameters of CuPc that is used. However, CuPc shows a relatively low dielectric constant ~ 4.85 , as reported by Voet and Suriani. [17] A large number of studies have been devoted to the improving of dielectric performance of the CuPc-based materials. Zhao synthesized a series of CuPc, which exhibits dielectric constants in the range of 3.95–6.81, using different reaction times [18]. Two series of hyperbranched CuPc are successfully synthesized, [19, 20] the dielectric constant of the

Electronic supplementary material The online version of this article (doi:10.1007/s10853-016-9785-y) contains supplementary material, which is available to authorized users.

✉ Renbo Wei
weirb10@uestc.edu.cn

✉ Xiaobo Liu
liuxb@uestc.edu.cn

¹ Research Branch of Advanced Functional Materials, Institute of Microelectronic & Solid State Electronic, High-Temperature Resistant Polymers and Composites Key Laboratory of Sichuan Province, University of Electronic Science & Technology of China, Chengdu 610054, People's Republic of China

hyperbranched CuPc with a thickness of 76 μm reaches 46 at 1 MHz and shows an extremely low dielectric dispersion [19]. GO has been shown to be an excellent additive for the improvement of dielectric performances of resin materials [21, 22]. However, to the best of our knowledge, improving of dielectric performance of the CuPc via covalent bonding with GO has not been reported in the literature yet.

In this paper, we report a facile and effective approach to prepare copper phthalocyanine/graphene oxide (CuPc-g-GO) nanohybrids via in situ polymerization. Isophorone diisocyanate (IPDI) and 3-aminophenoxyphthalonitrile (3-APN) are employed to functionalize GO with phthalonitrile moieties (GO-IPDI-CN), which are subsequently polymerized with 1,3,5-tri-(3,4-dicyanophenoxy) benzene (TPH) and CuCl, yielding the final hybrid CuPc-g-GO. The CuPc-g-GO is characterized by FTIR, TGA, DSC, XPS, SEM, UV–Vis, XRD, and AFM. The dielectric properties of CuPc-g-GO nanohybrids are also investigated in detail.

Experimental

Materials

Graphene oxide was purchased from XFANO Materials Tech Co.Ltd. (Nanjing, China). Isophorone diisocyanate (IPDI) and Stannous octoate were purchased from Shanghai Hengyi Co.Ltd. (Shanghai, China). TPH and 3-aminophenoxyphthalonitrile (3-APN) were synthesized in our laboratory according to the procedure described in the literature [23]. Cuprous chloride (CuCl), *N,N*-Dimethylacetamide (DMAc), and *N,N*-dimethylformamide (DMF) were purchased from Tianjin BODI chemicals, Tianjin, China. All the materials were used without any further purification.

Preparation of phthalonitrile moieties functionalized GO (GO-IPDI-CN)

GO (0.1 g) was firstly dispersed in DMF (100 mL) in a three-necked round bottom flask reactor and sonicated for 2 h. Then, IPDI (10 mL) was dropped into the reactor with vigorous stirring under N_2 atmosphere. The temperature of reactor was maintained at 50 $^\circ\text{C}$ for 7 h. After the reaction, the suspension was diluted with DMF (50 mL) and filtered over a 0.2- μm PTFE microporous membrane. The obtained GO-IPDI was ultrasonically dispersed in 100 mL of DMF for 0.5 h again. 10 g 3-APN and 2 drops of stannous octoate were added, and the system was stirred under nitrogen at 85 $^\circ\text{C}$ for 5 h. After the reaction, the suspension was diluted with 50 mL DMF and filtered over a 0.2- μm PTFE microporous membrane. The obtained phthalonitrile moieties-functionalized GO was washed thoroughly to remove the excess 3-APN and other impurities using DMF

with the assistance of sonication. After dried under vacuum overnight at 60 $^\circ\text{C}$, gray solid GO-IPDI-CN was finally obtained (as shown in Scheme 1).

Preparation of copper phthalocyanine grafted graphene oxide (CuPc-g-GO)

A weighted GO-IPDI-CN (0, 1, 5, 10 wt%) was added into 15 mL DMAc under sonication for 30 min. The obtained dispersion, as well as 0.5 g TPH and 47 mg CuCl was added to the flask equipped with a mechanical stirrer and refluxing condenser and reacted at 160 $^\circ\text{C}$ for 4 h. The mixture was poured into 100 mL of water. The crude product was collected by filtration, washed with water, and dried in vacuum. After refluxing in methanol twice, the product was filtrated and washed using cold methanol for three times. The final product was dried at 80 $^\circ\text{C}$ under vacuum overnight. According to the amounts of GO-IPDI-CN that was added, the final products were marked as CuPc, CuPc-g-GO1, CuPc-g-GO5, and CuPc-g-GO10, respectively.

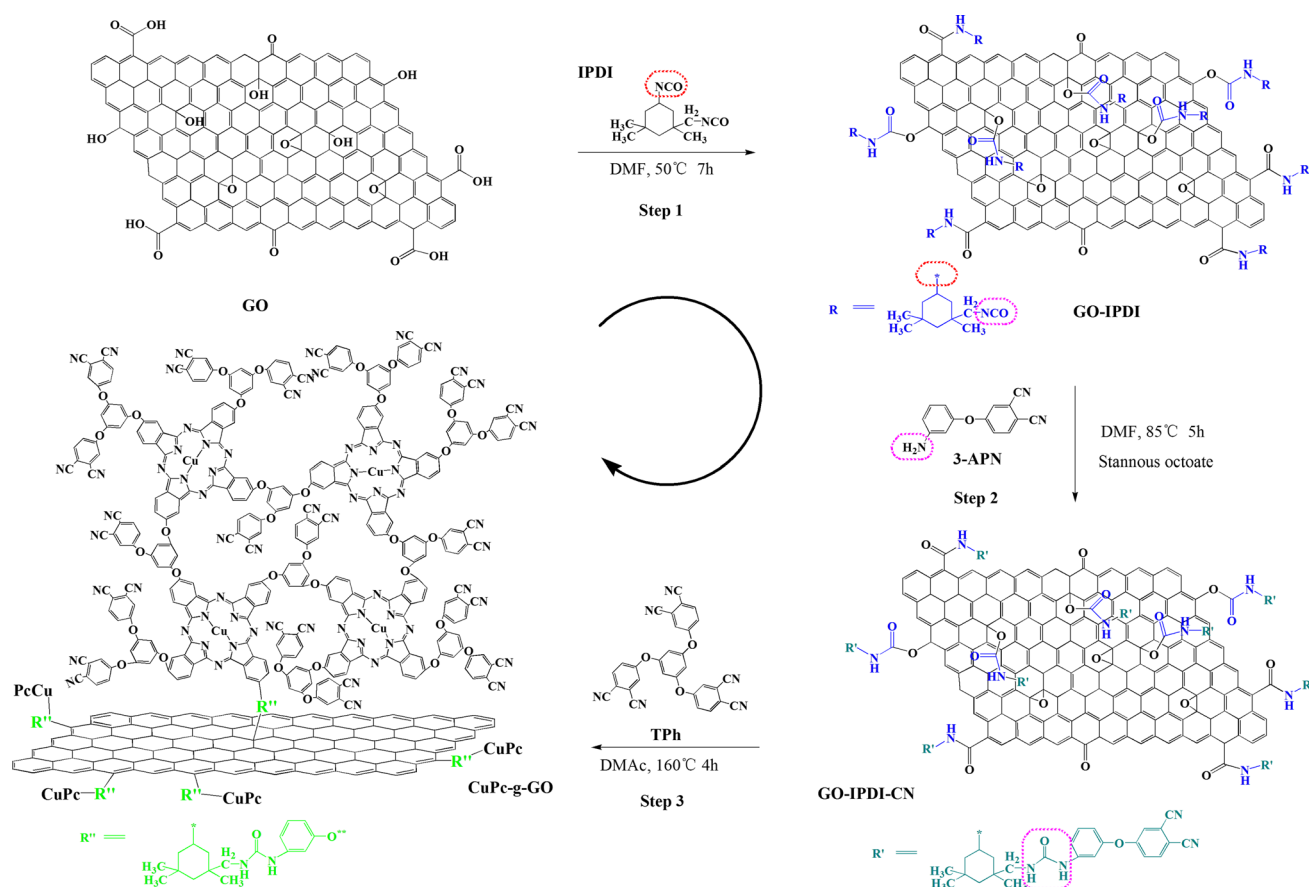
Characterization

Fourier transform infrared (FTIR) spectra were recorded with a Shimadzu 8400S (Shimadzu, Japan), FTIR spectrometer using KBr pellets between 4000 and 400 cm^{-1} in air. Thermogravimetry analysis (TGA) was conducted under N_2 atmosphere using a TA Instruments TGA Q-50 (TA Instruments, USA) at a heating rate of 20 $^\circ\text{C}/\text{min}$. DSC analysis was carried out under N_2 atmosphere at a heating rate of 10 $^\circ\text{C}/\text{min}$ using TA Q100 (TA Instruments, USA) series analyzer system. X-ray photoelectron spectroscopic (XPS) measurements were carried out on ESCA 2000 (VG Microtech, UK) using a monochromic $\text{Al K}\alpha$ ($h\nu = 1486.6$ eV) X-ray source. Scanning electron microscopic (SEM) images were taken on a JSM 6490LV (JEOL, Japan) field emission microscope. UV–Vis absorption spectra were recorded on a UV2501-PC spectrophotometer (Shimadzu, Japan). X-ray diffraction (XRD) was recorded on a RINT 2400 vertical goniometer (Rigaku, Japan) with Cu $\text{K}\alpha$ radiation. Atomic force microscopy (AFM) imaging was performed on a Digital Instruments multimode microscope controlled by Nanoscope III (Veeco, USA) equipped with a J scanner. Dielectric measurement was carried out by a dielectric analyzer (DEA 2970, TA Instrument, USA).

Results and discussion

Modification of GO

In order to characterize the structure of CuPc-g-GO and the intermediates, the FTIR spectra are measured and shown in



Scheme 1 The synthetic route of CuPc-g-GO

Fig. 1. The appearances of those characteristic absorption bands located at 3425 ($\nu_{\text{O-H}}$), 1725 ($\nu_{\text{C=O}}$), 1404 ($\delta_{\text{O-H}}$), 1220 ($\nu_{\text{epoxy C-O}}$), and 1055 cm^{-1} ($\nu_{\text{alkoxy C-O}}$) confirm the

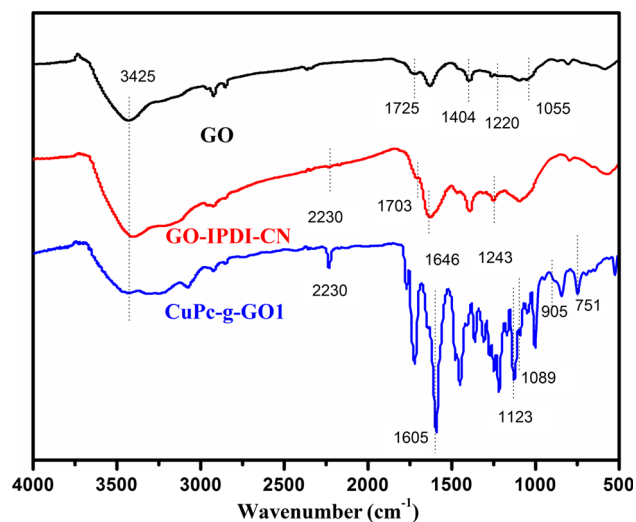


Fig. 1 FTIR spectra of GO, GO-IPDI-CN, and CuPc-g-GO1

existence of oxygen functional groups on the basal plane and edge of GO [24]. After reacting with IPDI and 3-APN, the absorption bands at 1725 and 1404 cm^{-1} disappear, and the new bands at 1703 (the carbonyl-stretching vibration of the carbamate esters of the surface hydroxyls), 1646 (an amide carbonyl-stretching mode) [25], and 1243 cm^{-1} (aromatic ether stretching vibration) are observed. Moreover, the new band at 2230 cm^{-1} is ascribed to the nitrile group, indicating that 3-APN is successfully grafted to the GO. As strong polar groups, nitrile groups will show cross-linking behavior in the presence of CuCl [26]. GO-IPDI-CN shows a characteristic exothermic peak on the DSC curve, corresponding to cross-linking reaction in the presence of CuCl around 305 °C (Fig. 2), which once again confirms the existence of the strong polar nitrile groups in GO-IPDI-CN [27, 28]. After the reaction with TPh, the copper phthalocyanine ring is formed as the new absorption peaks at 1605, 1123, 1089, 905, and 751 cm^{-1} , assigning to the phthalocyanine skeletal and metal–ligand vibration [29], are observed on the FTIR spectrum of CuPc-g-GO1.

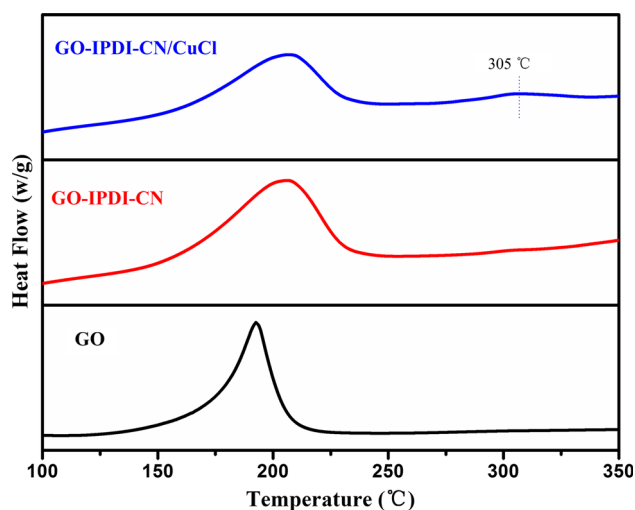


Fig. 2 DSC curves of GO, GO-IPDI-CN, and GO-IPDI-CN/CuCl

Thermal properties of the functionalized GO

TGA is further employed to confirm the grafting of CuPc on the surfaces of GO. GO suffers 30 % weight loss at the temperature range from 160 to 220 °C (Fig. 3), corresponding to the strong exothermic peak centered at 190 °C on the DSC curves. This is mainly attributed to the decomposition of labile oxygen functional groups, yielding CO, CO₂, and water vapor [30]. Upon reacting with IPDI and 3-APN, GO-IPDI-CN shows higher thermal stability, which can also be confirmed by the higher temperature of exothermic peak of GO-IPDI-CN on the DSC curve. IPDI and 3-APN alter the surface properties of GO, and prevent weight loss at low temperatures. Further heating from 180 to 400 °C, the thermal degradation of GO-IPDI-CN can be ascribed to the pyrolysis of the residual oxygen functional

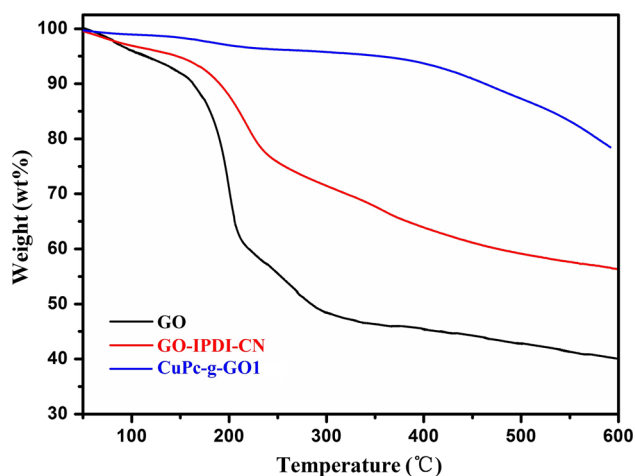


Fig. 3 TGA curves of GO, GO-IPDI-CN, and CuPc-g-GO1

groups and the decomposition of the isocyanates and aromatic ether [31]. Due to the formation of phthalocyanine ring structure, thermal stability of CuPc-g-GO1 is significantly improved as the temperature of 10 % weight loss of CuPc-g-GO1 is elevated from 190 °C (GO-IPDI-CN) to 471 °C (Fig. 3).

XPS spectra of the functionalized GO

Figure 4 shows the XPS spectra of GO, GO-IPDI-CN, and CuPc-g-GO1. Two obvious peaks are observed at 287 and 534.5 eV in the XPS spectrum of GO (Fig. 4a), corresponding to C1s and O1s, respectively. The C1s spectrum of GO could be quantitatively differentiated into four different carbon species (O=C–O, C=O, C–O, and C–C/C=C), as shown in Fig. 4b. After the reaction with IPDI and 3-APN, a significant decrease on the intensity of C–O peak at 286.6 eV is observed (Fig. 4c), indicating that hydroxyl groups on the surface of GO have been consumed by IPDI and are linked with the isocyanate. Furthermore, an additional component at 285.4 eV appears on the GO-IPDI-CN C1s spectrum (Fig. 4c), corresponding to C–N. N1s peak 400 eV is also observed after the modification with IPDI and 3-APN (Fig. 4a). The N1s core-level spectrum consists of two components with binding energies at 399.1 and 400.4 eV (Fig. 4d), corresponding to nitrile (CN) and amide (CONH) in GO-IPDI-CN [32, 33]. These results of XPS are consistent with that of FTIR. In addition, the content of nitrogen increases from 0 to 4.70 % for GO-IPDI-CN and further increases to 10.51 % for CuPc-g-GO1 (Table 1), confirming the successful grafting of IPDI, 3-APN, and CuPc. The decrease of content of oxygen and increase of content of carbon also prove the successful modification. Moreover, new slight reflection is found at 935.9 eV for the sample of CuPc-g-GO1, which is corresponding to Cu (II) (as shown in Fig. S1). The Cu element, deriving from the grafted CuPc, once again verifies the formation of CuPc.

Morphology properties of the functionalized GO

In order to investigate the influence of phthalonitrile functionalization and in situ polymerization of CuPc on morphology of the GO, SEM is used to observe the changes of microstructures of GO, GO-IPDI-CN, and CuPc-g-GO. As shown in Fig. 5a, GO consists of thin, flat, and randomly crumpled sheets. On the contrary, the edges and surfaces of GO-IPDI-CN appear relatively coarse after reacted with IPDI and 3-APN (Fig. 5b). Based on the reaction sites of IPDI and 3-APN, sheets with flocculent morphologies can be observed. Coarser edges and surfaces can be observed after the reaction with TPh (Fig. 5c),

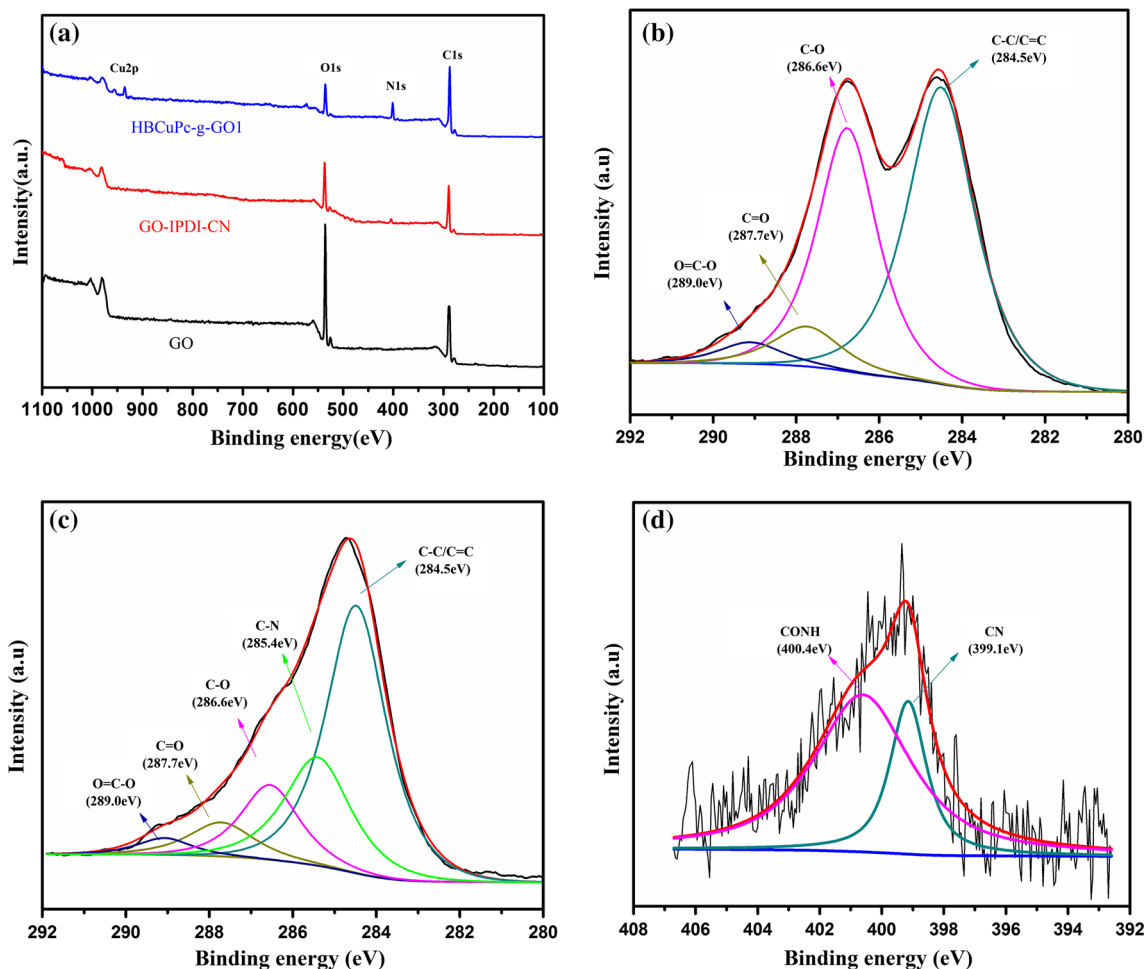


Fig. 4 XPS survey spectra of GO, GO-IPDI-CN, and CuPc-g-GO1 (**a**); **b** and **c** high-resolution XPS C1s core-level spectra of GO and GO-IPDI-CN, respectively, and **d** high-resolution XPS N1s of GO-IPDI-CN

Table 1 Atomic concentrations of GO, GO-IPDI-CN, and CuPc-g-GO1

Sample	C (wt%)	O (wt%)	N (wt%)	Cu (wt%)	C/O ratio
GO	67.07	32.93	0	0	2.04
GO-IPDI-CN	69.50	25.80	4.70	0	2.69
CuPc-g-GO1	74.64	14.07	10.51	0.78	5.30

indicating that CuPc is attached to the surface of GO nanosheets during the in situ polymerization process.

UV–Vis absorption spectra of the functionalized GO

Figure 6 shows UV–Vis spectra of GO, GO-IPDI-CN, CuPc-g-GO1, and CuPc in DMF. GO shows very broad absorption with continuously decreasing intensity from 265 to 800 nm. For GO-IPDI-CN, no adsorption peak is observed, indicating that the surface properties of GO have been changed after the reaction with IPDI and 3-APN. CuPc-g-GO1 shows two characteristic absorption bands at 550–750 and 250–350 nm, respectively, which confirms

the formation of copper phthalocyanine ring [28]. Compared with the spectrum of CuPc, it can be found that the Q-bands and shoulder peak shift from 611 and 677 to 619 and 684 nm, respectively. This red shift can be attributed to the strong π – π interaction between GO and grafted CuPc in CuPc-g-GO1, leading to the relocation of the electrons from graphene sheets to the copper phthalocyanine group in CuPc-g-GO1 [34].

XRD patterns of the functionalized GO

The structures of GO, GO-IPDI-CN, CuPc-g-GO1, and CuPc are further investigated by XRD. As shown in Fig. 7,

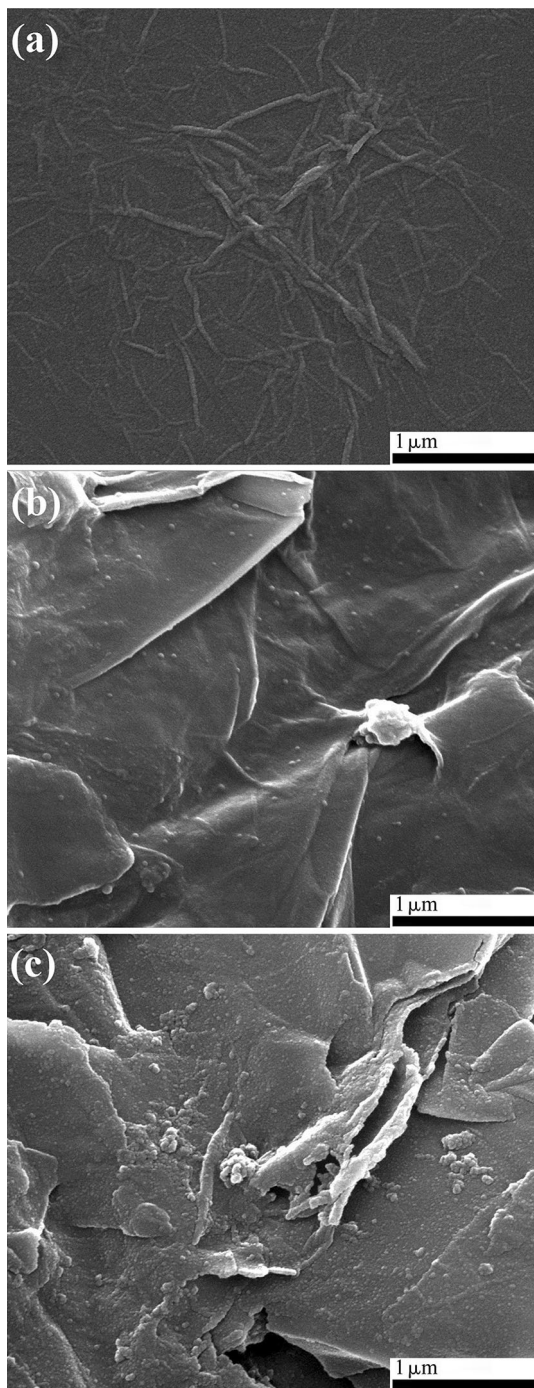


Fig. 5 SEM images of GO (a), GO-IPDI-CN (b), and CuPc-g-GO1(c)

the initial GO powder exhibits a sharp diffraction peak centered at $2\theta = 10.46^\circ$, corresponding to a d-spacing of 0.84 nm. After modification with IPDI and 3-APN, the diffraction peak of the GO-IPDI-CN shifts to a smaller position $2\theta = 7.88^\circ$, corresponding to a d-spacing of 1.12 nm. The increased interlayer spacing implies that

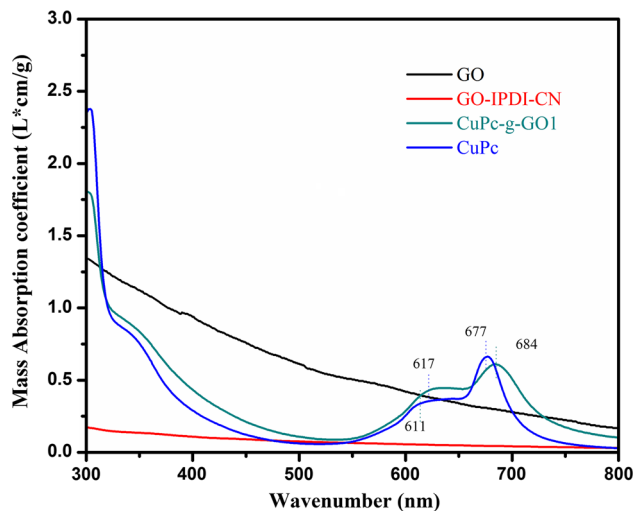


Fig. 6 UV-Vis absorption spectra of GO, GO-IPDI-CN, CuPc-g-GO1, and CuPc in DMF

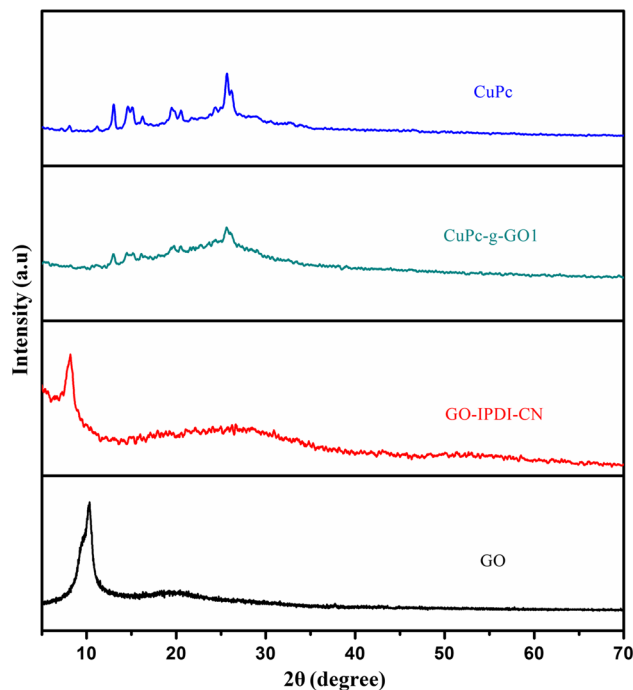


Fig. 7 XRD patterns of GO, GO-IPDI-CN, CuPc-g-GO1, and CuPc

IPDI and 3-APN are successfully inserted in GO and the layers of GO-IPDI-CN are further exfoliated. After the reaction between GO-IPDI-CN and TPh, the obtained CuPc-g-GO1 shows typical XRD pattern of CuPc, while there are no peaks of layer structure of GO-IPDI-CN, indicating that the GO is completely exfoliated by grafting CuPc [3]. The copper phthalocyanine crystallizes and the crystallite size of copper phthalocyanine in CuPc-g-GO1 is evaluated by means of Scherrer's equation of XRD peaks.

The average crystallite size of copper phthalocyanine in CuPc-g-GO1 is 20.8 nm (208 Å) as shown in the XRD fitting image of CuPc-g-GO1 in Jade 6 (Fig. S2). Meanwhile, the crystallite size of copper phthalocyanine in CuPc-g-GO1 also is measured in the following SEM image (Fig. S3), which is the same with the results of XRD.

AFM images of the functionalized GO

The typical surface morphologies of GO, GO-IPDI-CN, and CuPc-g-GO are characterized by AFM with the height profile, as shown in Fig. 8. It can be seen that the thickness of GO sheet is about 0.83 nm, corresponding to single layer. After introducing IPDI and 3-APN, the height of the single layer of GO-IPDI-CN becomes 2.16 nm, which is much higher than that of GO. The increase of thickness of GO-IPDI-CN mainly originates from the functionalization of GO sheet, leading to the extension of interlayer spacing of GO sheet. This result can be verified by the down-shift in the diffraction peak of GO-IPDI-CN in XRD spectrum. After the reaction between GO-IPDI-CN and TPh, the thickness of the obtained CuPc-g-GO1 reaches 25.31 nm, which once again confirms the results of crystallite size of CuPc in XRD. The obvious increase of the thickness for CuPc-g-GO1 could be attributed to the incorporation of CuPc on the surface of GO sheet. As the result of the extension in thickness of GO sheet, the diffraction peaks of layer structure of GO-IPDI-CN disappear in XRD, suggesting that the GO is further exfoliated.

Dielectric properties of the functionalized GO

The dielectric properties of CuPc-g-GO nanohybrids are measured as a function of frequency to study the effects of GO on the dielectric properties and alternating current (AC) conductivity of CuPc at room temperature. As shown in Fig. 9a, the dielectric constant of CuPc decreases slightly from 4 to 3.55 with frequency increasing from 100 Hz to 200 kHz. After being grafted to GO, the dielectric constant retains the same frequency dependence and shows a tendency to greatly increase with the increasing content of GO-IPDI-CN. The similar trend of dielectric loss and AC conductivity can also be observed in Fig. 9b and c. When the content of GO-IPDI-CN reaches 10 wt%, the dielectric constants at 100 Hz and 1 kHz are 9.04 and 8.16, with an increase of 116 and 103 % than that of the pure CuPc (4.21 and 4.02), respectively. The substantial improvement of the dielectric properties of the nanohybrids is attributed to the interfacial polarization, also known as Maxwell–Wagner–Sillars (MWS) polarization, between GO and CuPc [35]. High aspect ratios and large surface area of flake-like graphene oxide make it possible to form micro-capacitors combined with the grafting of CuPc. Interfacial polarization arises from electrical heterogeneous materials such as GO and CuPc in the micro-capacitors. The accumulation of charges and the formation of dipoles at the interfaces result in the increase of the dielectric constant. With the increasing content of GO-IPDI-CN, the number of micro-capacitors increases, leading to the formation of micro-capacitor

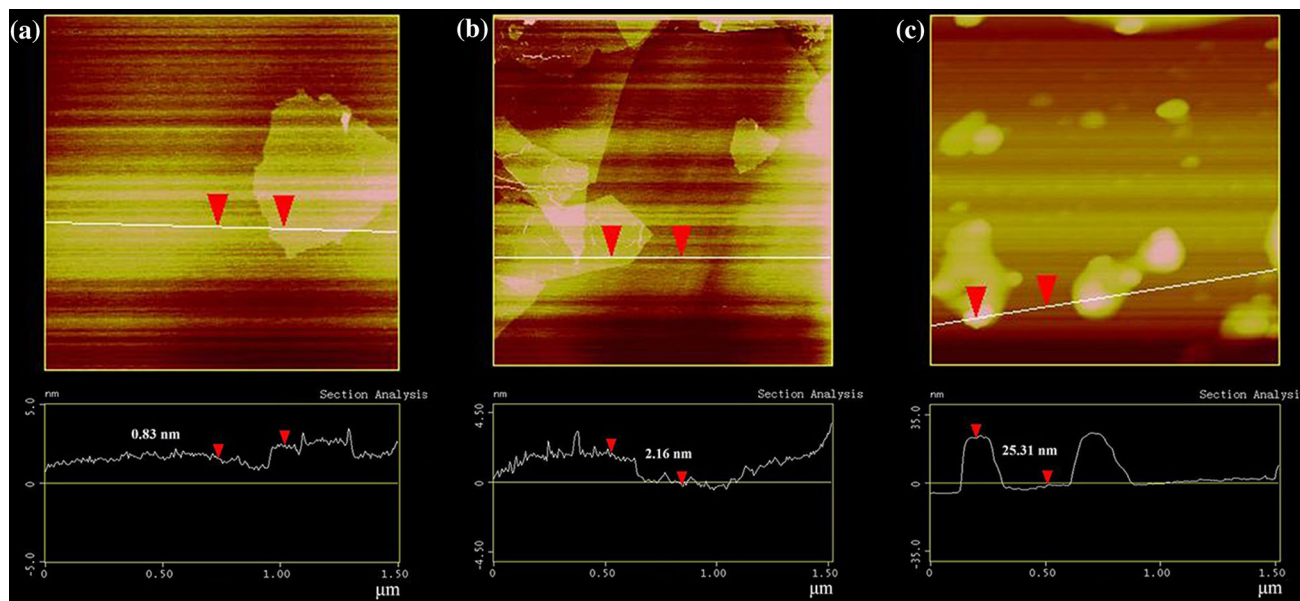


Fig. 8 AFM images of GO (a), GO-IPDI-CN (b) and CuPc-g-GO1 (c)

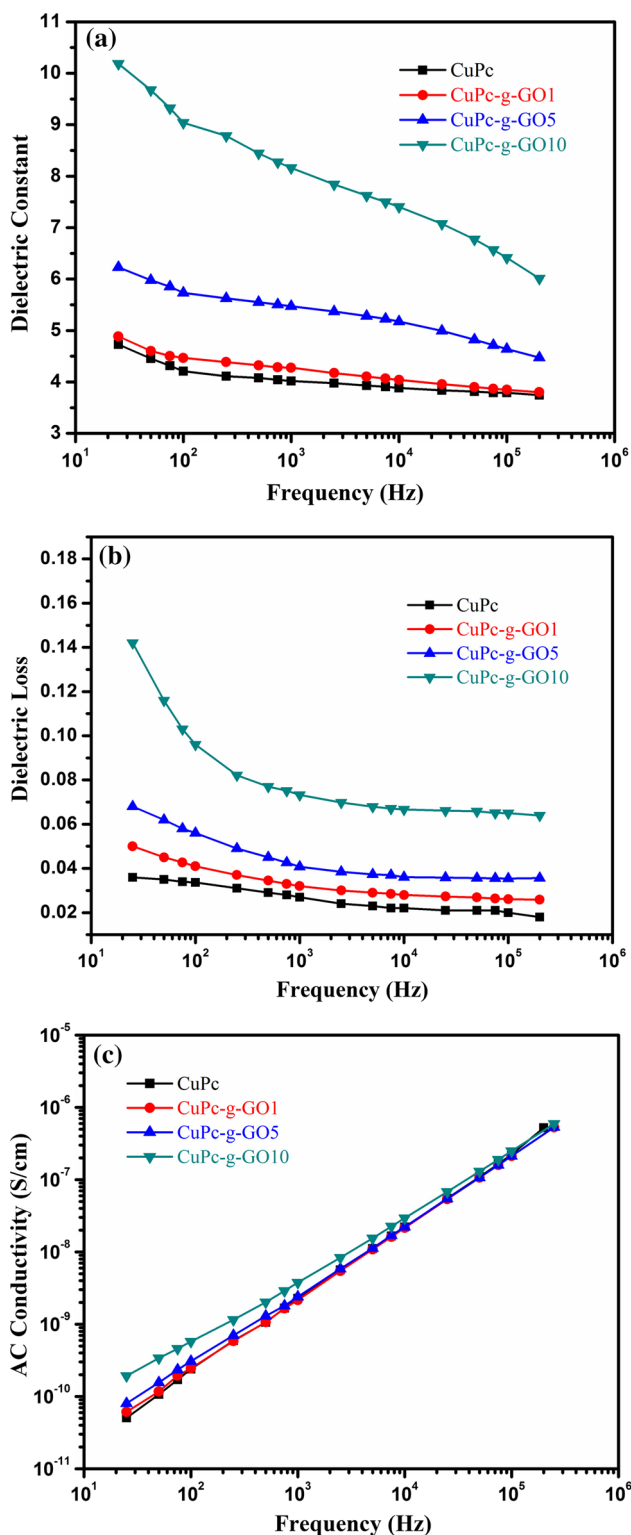


Fig. 9 Influence of GO-IPDI-CN content (0, 1, 5, 10 wt%,) on dielectric constant (a), dielectric loss (b), and AC conductivity (c) of CuPc-g-GO

network [36]. As a result, the dielectric constant increases significantly, when the content of GO-IPDI-CN goes beyond the percolation threshold.

Conclusions

In summary, novel CuPc-g-GO nanohybrids are successfully prepared via in situ polymerization. CuPc-g-GO nanohybrids and the intermediates were synthesized and characterized by FTIR, TGA, DSC, XPS, SEM, UV-Vis, XRD, and AFM. The results showed that the GO is completely exfoliated after the grafting of the CuPc. When the content of GO-IPDI-CN reaches 10 wt%, the dielectric constants at 100 Hz and 1 kHz are 9.04 and 8.16, with an increase of 116 and 103 % than that of pure CuPc (4.21 and 4.02), respectively. Such kinds of CuPc-g-GO will show great potential application as organic dielectric materials.

Acknowledgements The financial supports from National Natural Science Foundation of China (Project Nos. 51373028 and 51403029), “863” National Major Program of High Technology (2012AA03A212), South Wisdom Valley Innovative Research Team Program, and Ningbo Major (key) Science and Technology Research Plan (2013B06011) are gratefully acknowledged.

References

- Dreyer DR, Park S, Bielawski CW, Ruoff RS (2010) The chemistry of graphene oxide. *Chem Soc Rev* 39:228–240
- Wang JY, Yang SY, Huang YL, Tien HW, Chin WK, Ma CCM (2011) Preparation and properties of graphene oxide/polyimide composite films with low dielectric constant and ultrahigh strength via in situ polymerization. *J Mater Chem* 21:13569–13575
- Kim J, Im H, Kim JM, Kim J (2012) Thermal and electrical conductivity of Al(OH)₃ covered graphene oxide nanosheet/epoxy composites. *J Mater Sci* 47:1418–1426. doi:10.1007/s10853-011-5922-9
- Sun ST, Cao YW, Feng JC, Wu PY (2010) Click chemistry as a route for the immobilization of well-defined polystyrene onto graphene sheets. *J Mater Chem* 20:5605–5607
- Huang Y, Qin Y, Zhou Y, Niu H, Yu ZZ, Dong JY (2010) Polypropylene/graphene oxide nanocomposites prepared by in situ Ziegler-Natta polymerization. *Chem Mater* 22:4096–4102
- Bao CL, Guo YQQ, Song L, Kan YC, Qiana XD, Hu Y (2011) In situ preparation of functionalized graphene oxide/epoxy nanocomposites with effective reinforcements. *J Mater Chem* 21:13290–13298
- Tripathi SN, Saini P, Gupta D, Choudhary V (2013) Electrical and mechanical properties of PMMA/reduced graphene oxide nanocomposites prepared via in situ polymerization. *J Mater Sci* 48:6223–6232. doi:10.1007/s10853-013-7420-8
- Lu GH, Mao S, Park SG, Ruffand RS, Chen JH (2009) Facile, noncovalent decoration of graphene oxide sheets with nanocrystals. *Nano Res* 2:192–200
- Zhou N, Li J, Chen H, Liao C, Chen L (2013) A functional graphene oxide-ionic liquid composites-gold nanoparticle sensing platform for ultrasensitive electrochemical detection of Hg²⁺. *Analyst* 138:1091–1097
- de la Torre G, Claessens CG, Torres T (2007) Phthalocyanines: old dyes, new materials. Putting color in nanotechnology. *Chem Comm* 20:2000–2015
- Ma Z, Zhao R, Yang XL, Wei JJ, Meng FB, Liu XB (2012) Microwave absorption properties of Fe₃O₄/CuPc hybrid material

- with cooperative dual nonlinear dielectric/magnetic resonance. *Mater Lett* 69:30–33
12. Yang J, Yang XL, Pu ZJ, Chen L, Liu XB (2013) Controllable high dielectric permittivity of poly(arylene ether nitriles)/copper phthalocyanine functional nanohybrid films via chemical interaction. *Mater Lett* 93:199–202
 13. Choi S, Hong SH, Cho SH, Park S, Park SM, Kim O, Ree M (2008) High-performance programmable memory devices based on hyperbranched copper phthalocyanine polymer thin films. *Adv Mater* 20:1766–1771
 14. Lee TW, Kwon Y, Park JJ, Pu L, Hayakawa T, Kakimoto MA (2007) Novel hyperbranched phthalocyanine as a hole injection nanolayer in organic light-emitting diodes. *Macromol Rapid Commun* 28:1657–1662
 15. Wang Y, Li Z, Tian Y, Zhao W, Liu X, Yang J (2014) A facile way to fabricate graphene sheets on TiO₂ nanotube arrays for dye-sensitized solar cell applications. *J Mater Sci* 49:7991–7999. doi:10.1007/s10853-014-8506-7
 16. Li Y, Lu PF, Yan XZ, Jin L, Peng ZH (2013) Non-aggregated hyperbranched phthalocyanines: single molecular nanostructures for efficient semi-opaque photovoltaics. *RSC Adv* 3:545–558
 17. Voet A, Suriani LR (1952) Dielectric characteristics of pigment dispersions. *J Coll Sci* 7:1–10
 18. Zhao X, Zhao R, Yang XL, Zhong JC, Liu XB (2011) Synthesis and dielectric properties of hyperbranched CuPc based on biphenyl segments. *J Elect Mater* 10:2166–2171
 19. Guo M, Yan XZ, Kwon Y, Hayakawa T, Kakimoto M, Goodson T III (2006) High frequency dielectric response in a branched phthalocyanine. *J Am Chem Soc* 128:14820–14821
 20. Guo M, Hayakawa T, Kakimoto M, Goodson T III (2011) Organic macromolecular high dielectric constant materials: synthesis, characterization, and applications. *J Phys Chem B* 115:13419–13432
 21. Fan P, Wang L, Yang JT, Chen F, Zhong MQ (2012) Graphene/poly(vinylidene fluoride) composites with high dielectric constant and low percolation threshold. *Nanotechnology* 23:365702
 22. Wang ZC, Yang W, Liu XB (2014) Electrical properties of poly(arylene ether nitrile)/graphene nanocomposites prepared by in situ thermal reduction route. *J Polym Res* 21:358
 23. Guo H, Chen ZR, Zhang JD, Yang XL, Zhao R, Liu XB (2012) Self-promoted curing phthalonitrile with high glass transition temperature for advanced composites. *J Polym Res* 19(7):1–8
 24. Tang HX, Ehlert GJ, Lin YR, Sodano HA (2012) Highly efficient synthesis of graphene nanocomposites. *Nano Lett* 12:84–90
 25. Zhang B, Chen Y, Zhuang XD, Liu G, Yu B, Kang ET, Zhu JH, Li YX (2010) Poly (N-vinylcarbazole) chemically modified graphene oxide. *J Polym Sci Part A* 48:2642–2649
 26. Keller TM (1988) Phthalonitrile-based high temperature resin. *J Polym Sci* 26:3199–3212
 27. Yang XL, Zhan YQ, Yang J, Tang HL, Meng FB, Zhong JC, Zhao R, Liu XB (2012) Effect of nitrile functionalized graphene on the properties of poly(arylene ether nitrile) nanocomposites. *Polym Int* 61:880–887
 28. Wang ZC, Yang W, Wei JJ, Meng FB, Liu XB (2014) Preparation and microwave absorption properties of rod-like iron phthalocyanine with nitrile and nitro groups. *Mater Lett* 123:6–9
 29. Kobayashi T, Kurokawa F, Uyed N, Suito E (1970) The metal-ligand vibrations in the infrared spectra of various metal phthalocyanines. *Spectrochim Acta A* 26:1305–1311
 30. Alhassan MS, Qutubuddin S, Schiraldi AD, Agag T, Ishida H (2013) Dynamic puddle delineation and modeling of puddle-to-puddle filling spilling-merging-splitting overlaid flow processes. *Eur Polym J* 49:3825–3833
 31. Zhang DD, Zu SZ, Han BH (2009) Inorganic-organic hybrid porous materials based on graphite oxide sheets. *Carbon* 47:2993–3000
 32. Ramanathan T, Fisher FT, Ruoff RS, Brinson LC (2005) Amino-functionalized carbon nanotubes for binding to polymers and biological systems. *Chem Mater* 17:1290–1295
 33. Gammon WJ, Kraft O, Reilly AC, Holloway BC (2003) Experimental comparison of N1s X-ray photoelectron spectroscopy binding energies of hard and elastic amorphous carbon nitride films with reference organic compounds. *Carbon* 41:1917–1920
 34. Yang JH, Gao YJ, Zhang W, Tang P, Tan J, Lu AH, Ma D (2013) Cobalt phthalocyanine-graphene oxide nanocomposite: complicated mutual electronic interaction. *J Phys Chem C* 117:3785–3788
 35. Tsangaris GM, Psarras GC, Kouloumbi N (1998) Electric modulus and interfacial polarization in composite polymeric systems. *J Mater Sci* 33:2027–2037. doi:10.1023/A:1004398514901
 36. He F, Lau S, Chan HL, Fan JT (2009) High dielectric permittivity and low percolation threshold in nanocomposites based on poly(vinylidene fluoride) and exfoliated graphite nanoplates. *Adv Mater* 21:710–715